








## Article

# Eco-Friendly and Effective Diatomaceous Earth/Peat (DEP) Microbial Carriers in the Anaerobic Biodegradation of Food Waste Products

Agnieszka A. Pilarska <sup>1,\*</sup>, Krzysztof Pilarski <sup>2</sup>, Mariusz Adamski <sup>2</sup>, Maciej Zaborowicz <sup>2</sup>,  
Dorota Cais-Sokolińska <sup>3</sup>, Agnieszka Wolna-Maruwka <sup>4</sup> and Alicja Niewiadomska <sup>4</sup>

<sup>1</sup> Department of Hydraulic and Sanitary Engineering, Poznań University of Life Sciences, ul. Piątkowska 94A, 60-649 Poznań, Poland

<sup>2</sup> Department of Biosystems Engineering, Poznań University of Life Sciences, ul. Wojska Polskiego 50, 60-627 Poznań, Poland; pilarski@up.poznan.pl (K.P.); mariusz.adamski@up.poznan.pl (M.A.); maciej.zaborowicz@up.poznan.pl (M.Z.)

<sup>3</sup> Department of Dairy and Process Engineering, Poznań University of Life Sciences, ul. Wojska Polskiego 31, 60-624 Poznań, Poland; cais@up.poznan.pl

<sup>4</sup> Department of General and Environmental Microbiology, Poznań University of Life Sciences, ul. Szydlowska 50, 60-656 Poznań, Poland; amaruwka@up.poznan.pl (A.W.-M.); alicja.niewiadomska@up.poznan.pl (A.N.)

\* Correspondence: pilarska@up.poznan.pl; Tel.: +48-61-846-65-93

**Abstract:** This article aims to present the results of research on anaerobic digestion (AD) of waste wafers (WF-control) and co-substrate system—waste wafers and cheese (WFC-control), combined with digested sewage sludge. The aim of this study was to assess the physicochemical parameters of the diatomaceous earth/peat (DEP; 3:1) carrier material and to verify its impact on the enzymatic activity and the process performance. The experiment was conducted in a laboratory, in a periodical mode of operation of bioreactors, under mesophilic conditions. The results of analyses of morphological-dispersive, spectroscopic, adsorption, thermal, and microbiological properties confirmed that the tested carrier material can be an excellent option to implement in biotechnological processes, especially in anaerobic digestion. As part of the experiment, the substrates, feedstock, and fermenting slurry were subjected to the analysis for standard process parameters. Monitoring of the course of AD was performed by measuring the values of key parameters for the recognition of the stability of the process: pH, VFA/TA ratio (volatile fatty acids/total alkalinity), the content of  $\text{NH}_4^+$ , and dehydrogenase activity, as an indicator of the intensity of respiratory metabolism of microorganisms. No significant signals of destabilization of the AD process were registered. The highest dehydrogenase activity, in the course of the process, was maintained in the WFC + DEP system. The microbial carrier DEP, used for the first time in the anaerobic digestion, had a positive effect on the yield of methane production. As a result, an increase in the volume of produced biogas was obtained for samples fermented with DEP carrier material for WF + DEP by 13.18% to a cumulative methane yield of  $411.04 \text{ m}^3 \text{ Mg}^{-1} \text{ VS}$ , while for WFC + DEP by 12.85% to  $473.91 \text{ m}^3 \text{ Mg}^{-1} \text{ VS}$ .

**Keywords:** diatomaceous earth/peat carrier; physicochemical properties; anaerobic biodegradation; food waste; process efficiency



**Citation:** Pilarska, A.A.; Pilarski, K.; Adamski, M.; Zaborowicz, M.; Cais-Sokolińska, D.; Wolna-Maruwka, A.; Niewiadomska, A. Eco-Friendly and Effective Diatomaceous Earth/Peat (DEP) Microbial Carriers in the Anaerobic Biodegradation of Food Waste Products. *Energies* **2022**, *15*, 3442. <https://doi.org/10.3390/en15093442>

Academic Editor: Byong-Hun Jeon

Received: 1 April 2022

Accepted: 5 May 2022

Published: 9 May 2022

**Publisher's Note:** MDPI stays neutral with regard to jurisdictional claims in published maps and institutional affiliations.



**Copyright:** © 2022 by the authors. Licensee MDPI, Basel, Switzerland. This article is an open access article distributed under the terms and conditions of the Creative Commons Attribution (CC BY) license (<https://creativecommons.org/licenses/by/4.0/>).

## 1. Introduction

Anaerobic digestion process (AD) is a biotechnological process widely used in the treatment of organic waste of various origins, leading to the production of value-added products such as biogas and biofertilizer in the form of post-fermentation pulp [1]. Presently, advanced research on the AD of food waste (FW) is being undertaken in many research centers around the world to improve process efficiency [2–4]. According to the results of studies on anaerobic co-digestion (AcoD) of FW, the inclusion of this type of waste

is beneficial for methane yield and the kinetics of the process, while the fermentation of individual substrate is often volatile. The beneficial effects observed by the researchers were mainly related to the balanced availability of macro- and micro-nutrients, buffer capacity, and dilution of inhibitory compounds [5,6]. An effective co-substrate should have a complementary composition to the basic substrate and induce synergistic effects [7]. As evidenced by previous research by Pilarska et al. (2019, 2021), the materials that meet the above-mentioned conditions are confectionery waste and cheese waste [8,9]. The confectionery industry constantly produces waste [10–12]. The physicochemical properties of confectionery waste and its composition contribute to a high biochemical methane potential (BMP), while dairy waste acts as a process buffer and is a source of numerous minerals.

Immobilization is a method of immobilizing the microbial or plant cells in a suitable material [13–15]. The most important characteristics of carrier material suitable for a given process are its biocompatibility, porosity, chemical, mechanical and thermal stability, availability, and low cost [16,17]. Based on the literature on the subject, several types of carrier materials have been tested in the methane fermentation process so far, e.g., natural zeolites—due to their favorable characteristics for microorganism adhesion, but also granulated polymeric support [poly(acrylonitrile-acrylamide)], rubberized-coir, clay (morillonite and bentonite), glass beads, microcarriers, membranes, granulated activated carbon, wood shavings, silica, lignin, etc. [18–21]. The improvement in methane or hydrogen production is attributed to the action of cell immobilization materials, consisting in reducing the release and impact of inhibitors, making immobilized cells insensitive to changes in environmental conditions, stabilizing the system and increasing the biodegradability of substrates.

An excellent option for use as a bacterial carrier material in methane fermentation is diatomaceous earth (diatomite) which is an organogenic rock formed mainly from the shells of diatoms (single-celled algae) found in marine and lake soils. It may also contain remains of other organisms, detrital quartz and calcite, glauconite, clay substances, and iron compounds [22–24]. Diatoms have a porous, well-structured cell wall, called frustule, the function of which is to protect them from environmental stress. Frustule is an excellent and cheap source of biosilica, which thanks to its high biocompatibility, porosity, and a well-developed surface, is widely used in regenerative medicine and as a drug carrier material [25–27]. Due to its chemical composition and properties, diatomaceous earth is widely used in many industries [28]. Janićijević et al. (2015), in their experiment, used refined diatomite as adsorbent for diclofenac sodium, which enabled the preparation of comprimates containing a therapeutic dose of the adsorbed drug [29]. The high thermal stability of diatomite was taken advantage of while using it as a carrier to improve the thermal properties of medium- and high-temperature PCMs (Phase Change Materials) [30]. Based on the literature on the subject, diatomaceous earth can also be used as: a base ingredient of magnetic polyvinyl alcohol-sodium alginate-diatomite (PVA-SA-diatomite), composite carriers for immobilized microorganisms prepared for removal of NH-N from effluents [31], a substitute for cement, to improve the compressive strength and absorbability of mortar [32], and insecticide, since the results of the research conducted in that field confirm that DE can be a practical alternative to synthetic pesticides in some applications [33]. Other innovative applications of natural diatomite might be its use as an effective solid catalyst for the production of biodiesel [34], a support material to speed up the granulation process of aerobic granular sludge (AGS) in a pilot sequencing batch reactor (SBR) for domestic wastewater treatment [35], and also as a filtering agent (e.g., in brewing), bleaching agent, dewatering agent, refractory material, thermal, acoustic, and electrical insulation [24,36].

With regards to the use of the basic component of natural diatomite, silica, Pilarska et al., 2020, 2021, in their previous articles, presented the efficiency of anaerobic digestion of organic waste carried out with the use of the silica/lignin system (4:1) as cell carrier materials [9,21]. The addition of silica had a key effect on increased bacterial proliferation and enzymatic activity, which directly contributed to an increase in biomass conversion and process efficiency (by approx. 18%). It should be added that diatomite can be as effective a carrier material as silica, and it is cheaper. The recent research in that field, presented by

Zhang et al., 2021, is an interesting proposal for an innovative technology that makes use of diatomite to increase the production of methane in the process of anaerobic digestion of algae [37]. According to the authors' research report, in the experiment of continuous operation of the fermentation chamber, conducted for 136 days, the daily methane efficiency increased by approx. 31% as a result of the addition of diatomite ( $5 \text{ g} \cdot \text{L}^{-1}$ ).

In turn, peat, which was used as a minor component of the cell carrier material in this study, is the preferred carrier material in agricultural applications. This substrate has been also used as a carrier to formulate plant growth promoting rhizobacteria (PGPR) or a biocontrol agent [38]. It consists of undecomposed parts of plants and an amorphous substance—humus. Depending on which component predominates, peat can vary in structure. The more plant debris, the more fibrous it is [39]. As the humus content increases, it becomes plastic and amorphous. Peat also contains mineral substances. The active component of the organic matter, humus, is characterized by high hydrophilicity and sorption capacity, therefore peat is often also used as an adsorbent. The sorption properties of peat are related to the presence of acid functional groups on its surface (carboxyl  $\text{ACOOH}$ , phenolic  $\text{AOH}$ , sulfonic  $\text{ASO}_3\text{H}$ ), thanks to which it can easily adsorb positively charged metal ions, through exchange with  $\text{H}^+$  ions. The conducted research confirms the effectiveness of removing, i.e., nickel(II) and lead(II) ions from aqueous solution using peat as a cheap adsorbent [40]. Peat is widely used as a growing medium in soilless systems, where it performs basic functions such as plant anchoring and supply of dissolved substances, water, and oxygen, as well as a material to obtain peat extracts as a humic product for the improvement of soil [41,42].

The aim of the study was to assess the impact of a microbial medium in the form of the diatomaceous earth/peat (DEP) (3:1) system, which has not been used in the AD process so far, on the enzymatic activity and process performance in laboratory-scale anaerobic digesters. The cumulative methane yield was determined for samples with wafers (WF) and co-substrates of wafers and cheese (WFC) as control variants, and for analogous samples with a carrier material. The performed experiment was successful due to the physicochemical and microstructural properties of the compounds that formed the carrier material.

## 2. Materials and Methods

### 2.1. Substrate and Carriers

In the presented research, the substrates were waste wafers (WF) with filling and waste cottage cheese (CHE), collected from manufacturing companies located in the vicinity of Poznań. As inoculum, similarly to the previous experiments, digested SS (sewage sludge) was used, collected from a municipal sewage treatment plant, which is also an effective buffer for the system.

Two materials were used as components of diatomaceous earth/peat (3:1) samples: diatomaceous earth, diatomite, 15 g (Perma-Guard, Inc., Bountiful, UT, USA) and 5 g of deacidified peat (Torf Corporation Sp. z o.o., Wrocław, Poland), a dose per 1 L of the feedstock. Diatomite used in the study was 100% diatomaceous earth of freshwater origin with a high specific surface area, the so-called amorphous silica (see Figure 1a).

Before use, peat was dried for 24 h in a stationary dryer at  $105^\circ\text{C}$  (SUP-18W dryer by Wamed, Warsaw, Poland) to remove physically bound water (Figure 1b) and then, it was ground thoroughly with the use of a porcelain mortar.

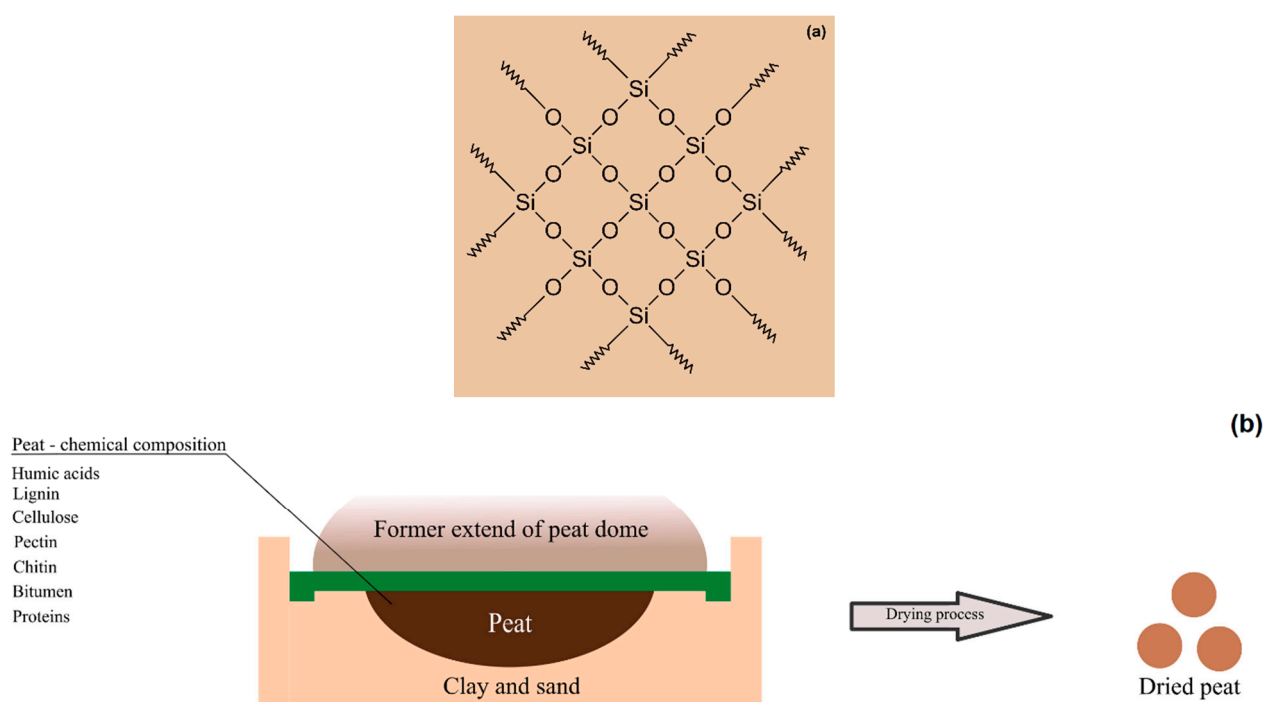


**Figure 1.** (a) Structural formula of silica as the basic component of diatomaceous earth and (b) the process of removal of water from peat by drying, taking into account the cross-section of the peat bed (authors' own graphics).

## 2.2. Biogas Production Set-Up

### 2.2.1. Batch Preparation

In this study, control samples of WF-control (waste wafers), WFC-control (co-substrates of waste wafers and cheese) and samples with the addition of DEP carrier, WF + DEP and WFC + DEP, were tested. The amount of substrates and inoculum was determined according to the standard VDI 4630 [43]; the proportions of the mixture were set, so that the content of total solids did not exceed 10% [44]. The composition of the samples and their physicochemical parameters is presented in Table 1.

**Table 1.** Composition and parameters of the substrate/inoculum samples.

Samples	WF (g)	CE (g)	Carrier (g)	Inoculum (g)	pH	TS (%)	VS (%)
WF-control	9.8	-	-	830.2	7.15	4.00	72.50
WF + DEP	9.8	-	20.0	830.3	7.03	3.96	70.62
WFC-control	5.5	2.9	-	832.6	6.96	3.75	70.38
WFC + DEP	5.6	2.9	20.0	832.5	6.85	3.72	68.55

### 2.2.2. Anaerobic Digestion

Anaerobic digestion (AD) was performed in a bioreactor, presented in Figure 2. The total number of fermentation chambers in the experiment was 12. The 1.0 L bioreactors (5) were filled with a substance that was stirred once a day. The bioreactors were placed in a container with water (4), connected to a heater (1), which allowed to perform the process at a set range of temperatures (mesophilic conditions). The produced biogas was directed (7) into tanks (8) (with a scale) where it was stored.

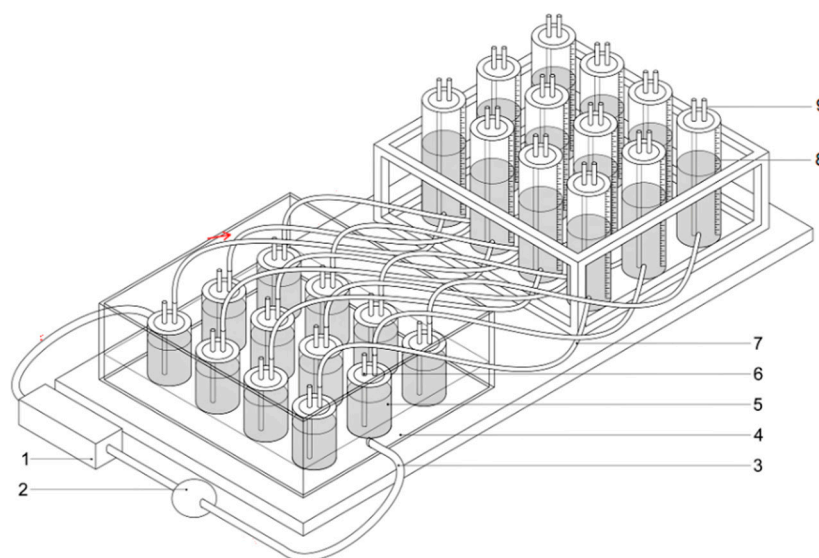


**Figure 2.** The bioreactor (12-chamber section) used in biogas production experiment: 1—water heater; 2—water pump; 3—insulated tubes for heating medium; 4—water jacket (39 °C); 5—bioreactor (1.4 L); 6—slurry sampling valve; 7—tube for biogas transport; 8—graduated tank for biogas; 9—gas sampling valve (Adapted with permission from Ref. [12]. 2019, Molecules, Multidisciplinary Digital Publishing Institute, Basel, Switzerland).

The hydraulic retention time (HRT) was 21 days. As per the German standard DIN Guideline 38 414-S8 (Deutsches Institut für Normung) [44], the experiment was performed until daily production of biogas dropped below 1% of the total biogas produced. The concentration of methane, carbon dioxide and other gases (forming biogas) was measured with the Geotech GA5000 gas instrument (Coventry, UK). The total amount of biogas was calculated with the use of formulas that had been described in the previous articles [3,4,45].

### 2.3. Analytical Methods

#### 2.3.1. Physicochemical Research of the Carrier

In this study, a comparative analysis of the morphological-dispersive and physico-chemical properties of the components of the diatomaceous earth/peat carrier material and the system as a whole was performed.

The microstructure of the kraft lignin and kraft lignin/silica materials were examined on the basis of SEM (scanning electron microscope) images recorded from a scanning electron microscope, FEI Quanta FEG 250 (Thermo Fisher Scientific, Waltham, MA, USA). The microscope operates in Low Vacuum mode at 70 Pa using an accelerating voltage of 10 kV. Before testing, the samples were coated with Au for a time of 5 s using a Balzers PV205P coater (Oerlikon Balzers Coating S.A., Brugg, Switzerland) [15].

To determine the porous structure parameters, nitrogen adsorption/desorption isotherms at 77 K and parameters such as surface area ( $A_{BET}$ ), total volume ( $V_p$ ), and mean size ( $S_p$ ) of pores were determined using an ASAP 2420 instrument (Micromeritics Instrument Co., Norcross, GA, USA). Prior degas were performed at the temperature of 90 °C in vacuum conditions.

Fourier transform infrared spectroscopy (FT-IR) measurements were performed on a Vertex 70 spectrophotometer (Bruker, Bremen, Germany) at room temperature. The sample was analyzed, in the form of tablets, made by pressing a mixture of anhydrous KBr (ca. 0.25 g) and 1 mg of the tested substance in a special steel ring under a pressure of approximately 10 MPa. FT-IR spectra were obtained in the transmission mode between 4000 and 400  $\text{cm}^{-1}$ . The analysis was performed at a resolution of 0.5  $\text{cm}^{-1}$  [21].

The chemical composition of the samples was determined using an elemental analyzer, FLASH 2000 (Thermo Fisher Scientific, Waltham, MA, USA), which operates based on



dynamic combustion technology. Samples (approximately 2–4 mg) were placed in the reactor using an autosampler, together with a strictly-defined portion of oxygen. After combustion at 900–1000 °C, the exhaust gases were transported in helium flow to the second furnace of the reactor, filled with copper and then, through a water trap, to the chromatography column. Finally, the separated gases were detected using the Thermal Conductivity Detector [15].

### 2.3.2. Physicochemical Analysis of Substrate and Samples

Substrates and samples were subjected to pH analysis (potentiometric analysis) and electrolytic conductivity with an Elmetron CP-215 apparatus (ELMETRON, Zabrze, Poland). Total solids (TS) were measured by drying at 105 °C (Zalmed SML dryer, Zalmed, Łomianki, Poland) and volatile solids (VS) by combustion at 550 °C (MS Spectrum PAF 110/6 furnace, MS Spectrum, Warsaw, Poland).

The substrates and fermented materials were tested for their carbon content. For this purpose, a process of combustion was performed at 900 °C and then, CO<sub>2</sub> determination (Infrared Spectrometry, OI Analytical Aurora 1030W TOC Analyzer, Picarro Inc., Santa Clara, CA, USA). The content of nitrogen was also checked—titration, Kjeldahl method, using 0.1 n HCl, in the presence of Tashiro's indicator and ammonium nitrogen—and the distillation and titration method using 0.1 n HCl, in the presence of Tashiro's indicator [12].

Also, the content of VFA (volatile fatty acids) and TA (total alkalinity) and then the VFA/TA ratio (volatile fatty acids to total alkalinity ratio) in the fermenting feedstock were determined. A total of 5 mL of the sample was collected, titrated by 0.1 N of sulfuric acid solution (H<sub>2</sub>SO<sub>4</sub>) up to pH 5.0, to calculate the TA value. The VFA value was obtained after a second titration step between pH 5.0 and pH 4.4 [8].

### 2.3.3. Biochemical Analysis of Digestate

The samples underwent biochemical analysis (dehydrogenase activity, DHA) by means of the spectrophotometric method [46]. Samples (5 mL) were incubated at 30 °C, at a pH of 7.4 for 24 h along with 2,3,5-triphenyltetrazolium chloride (TTC). Triphenylformazan (TPF) was obtained, extracted with 96% ethanol, and measured using a spectrophotometer at 285 nm. The dehydrogenase activity was expressed as  $\mu\text{mol TPF mL}^{-1} \text{ DM of waste } 24 \text{ h}^{-1}$ .

### 2.3.4. *Bacillus Amyloliquefaciens* Biomass Determination

The biomass of bacterial cells with the tested DEP carrier was determined by weighing. First, the prepared carrier was rinsed with PBS solution and dried at 70 °C to a constant initial mass (SUP-18W dryer by Wamed, Warsaw, Poland). Then, the carrier, in the amount calculated per 100 mL (see Section 2.1) was mixed in a flask with 0.6 g of glucose and 1.3 g of regular broth, and supplemented with distilled water to a volume of 100 mL, sterilized in an autoclave for 40 min at 110 °C. On the prepared substrate, an autochthonous strain of bacteria *Bacillus amyloliquefaciens* was placed, isolated from fermented sewage sludge [9]. Inoculated samples were incubated at 24 °C for 5 days in an incubator (Compact Shaker KS 15 B-Edmund Bühler GmbH, Bodelshausen, Germany) and shaken (75 rpm). After 5 days, the cultures, including control samples, were centrifuged (15,000 rpm, 15 min) with the use of a Hettich Universal 16 R centrifuge (Hettich Holding GmbH & Co. oHG, Kirchlingern, Germany). The biomass of cells, grown on the substrate along with the carriers, was determined as the difference in weight (g) of the uninoculated substrate and the substrate inoculated with an autochthonous strain of bacteria *Bacillus amyloliquefaciens*.

Statistical analyses were performed with Statistica 13.3 software (StatSoft Inc. 2013, Tulsa, OK, USA). Two-way ANOVA was applied to determine the significance of the variation in the enzymatic activity. Tukey's test was performed to calculate homogeneous mean subsets at a level of significance of  $p < 0.05$ . Principal Component Analysis was performed using Past 3.25 software (Oslo, Norway).

### 3. Results and Discussion

#### 3.1. Feedstock and Inoculum Characterisation

Waste wafers (WF) and cheese (CHF) were selected by the author of the study to test the carrier materials in anaerobic digestion (AD), as stand-alone substrates and in a co-substrate system, due to their high biochemical methane potential (BMP) determined by the significant content of organic matter (See Table 2; volatile solids, VS). Waste wafers, similarly to other types of confectionery waste [12], are characterized by the high content of total solids (TS). In turn, waste cheese, as indicated by the results in Table 2, is characterized by high conductivity (Table 2) due to the significant content of minerals [3]. A significant content of carbon is related to the fat present in curd, while the content of nitrogen—to the protein found in dairy products [47]. The share of ammonium nitrogen in the values presented in Table 2, in both waste wafers and cheese, does not qualify  $\text{N-NH}_4$  as a potential process inhibitor [48]. The acidic pH value of cheese waste may raise concerns with regards to the stability of its anaerobic treatment, and so can the salt it contains. Taking the above into account, the author of the study introduced (as the first person so far, considering the data in the literature on the subject) a combination of both WF and CHE waste (WFC system). A clear synergistic effect was confirmed by microbiological and biochemical analyses (increase in cell counts and enzymatic activity in the system) [7,8]. The chemical composition of waste wafers and cheese was described in detail by the author of the study in the previous publications.

**Table 2.** Physicochemical parameters of feedstock and inoculum.

Waste	pH	Cond.	TS	VS	C/N Ratio	C	N	N-NH <sub>4</sub>
	-	(mS cm <sup>-1</sup> )	(wt %)	(wt % <sub>TS</sub> )	-	(wt % <sub>TS</sub> )	(wt % <sub>TS</sub> )	(wt % <sub>TS</sub> )
Wafers	7.15	2.92	84.73	95.32	50.92	46.85	0.92	0.43
Cheese	4.86	94.36	28.21	98.41	3.22	52.47	16.31	0.69
Inoc.	7.23	44.08	2.17	72.55	5.96	35.72	5.99	2.95

Cond. = conductivity, TS = total solids, VS = volatile solids, Inoc. = inoculum.

The digested sewage sludge, used by Pilarska et al. in the successive experiments, apart from its inoculum function, also acted as a buffering factor, thanks to which the performed biodegradation processes were stable, characterized by high efficiency—similar to the theoretical BMP [3,6,21,45]. As the author of the study explains in one of her previous publications, digested SS is characterized by its high alkalinity due to carbonates and bicarbonates released during the anaerobic digestion of raw sewage sludge. The previous studies indicate an almost fivefold increase in the alkalinity of SS as a result of anaerobic biodegradation [45].

#### 3.2. Diatomaceous Earth/Peat Properties and Productivity

##### 3.2.1. FT-IR Spectra and Elemental Analysis

The raw diatomite from the deposit is characterized by a 72% concentration of  $\text{SiO}_2$  (see Figure 1). An interesting fact is that diatomite with silica content above 80% is not found in Poland [22]. The mass-averaged quantitative and qualitative elemental analysis of EDS (energy-dispersive X-ray spectroscopy) showed that the key elements in diatomaceous earth are: oxygen (48.4%), silicon (45.7%), aluminum (3.2%), and iron (2.7%). The result concerning the percentage content of oxygen is consistent with the results of the tests performed by the author of the study, presented in Table S1 (see Supplementary Materials).

When analyzing the FT-IR spectrum (Fourier Transform-Infrared) presented in Figure 3, the peak at  $466\text{ cm}^{-1}$  represents the bending vibration of the Si–O group (both in lighter and darker color); the peak at  $800\text{ cm}^{-1}$  indicates the vibration of SiO–H group; and the peak around  $1103\text{ cm}^{-1}$  belongs to the stretching vibration of siloxane (–Si–O–Si–) group. Moreover, the stretching vibration and the bending vibration of the single-bond –OH functional group were found at the wave number of  $1639$  and  $3430\text{ cm}^{-1}$ , respectively. As

can be seen from Figure 3, the pure diatomite possesses the main absorption bands at 3430, 1639, 1429, 1103, 800, and 466  $\text{cm}^{-1}$  and it is consistent with the data in the literature on the subject [30,49,50]. All of these characteristic peaks suggest that diatomite is mainly composed of  $\text{SiO}_2$ . Small peaks at 697, 1639, 1875  $\text{cm}^{-1}$  in the IR spectra of DE probably originated from, inter alia,  $\text{Si}\backslash\text{O}\backslash\text{Al}$  vibrations (peak at 697  $\text{cm}^{-1}$ ), which suggests the presence of small amounts of clay impurities (minerals composed of hydrated aluminum, magnesium, and iron aluminosilicates) were present in the diatomite sample [29,51].

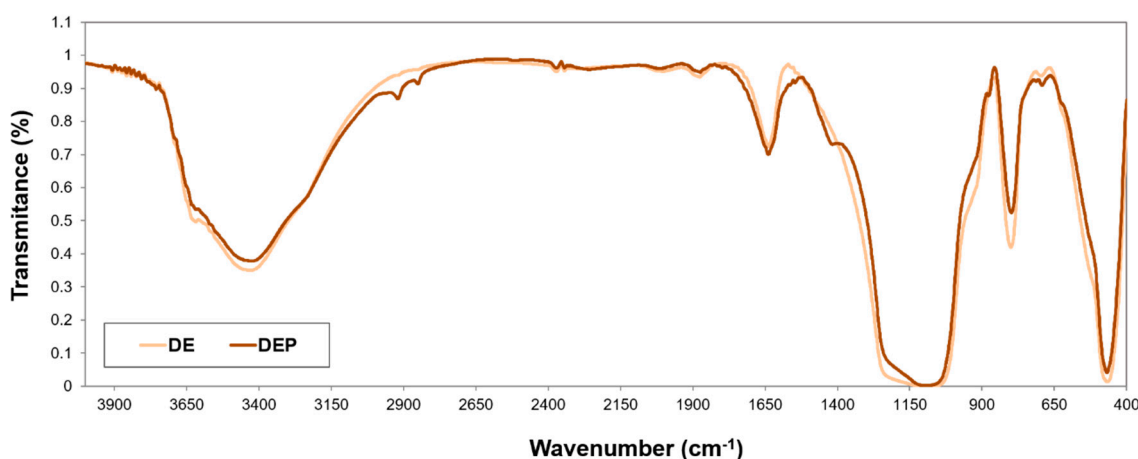


**Figure 3.** FT-IR spectrum of DE (diatomaceous earth) and DEP (diatomaceous earth/peat, 3:1) samples.

As per the data in the literature, peat is an organic material with a high water content (88–92%), typically consisting of carbon (50–60%), hydrogen (5–7%), nitrogen (2–3%), phosphorus (<0.2%), oxygen, and mineral nutritional elements, which is consistent with the results obtained (see Table S1, Supplementary Materials). Cannavo et al. (2013), in their study, defined peat as a heterogeneous, complex mixture of organic humic acids and their salts, bitumens, and carbohydrates, including pectin, cellulose, chitin, lignin, and proteins (see Figure 1) [52]. The publications of other scientists contain detailed analyses of the FT-IR spectrum of peat, confirming the diversity of natural composition of peat and the presence of characteristic functional groups in its structure, including: hydroxyl groups, O–H; ether groups, C–O; and carbonyl groups, C=O. The presence of a developed aliphatic structure was confirmed by the absorption band derived from the stretching vibrations of C–H bonds [40,53].

As described above, the FT-IR spectrum for the diatomaceous earth/peat system, 3:1 (see Figure 3), apart from the previously discussed clear bands corresponding to the groups characteristic for diatomite, has bands that may originate from peat. For example, the visible peak at 1418  $\text{cm}^{-1}$  that comes from the stretching vibrations of C–OH groups, or the peaks at the values of 2851 and 2919  $\text{cm}^{-1}$  attributed to the vibrations of C–H bonds.

### 3.2.2. Dispersive and Morphological Properties

Unmodified diatomaceous earth (DE) is characterized by a rich diversity in particle size and shape and consists mainly of broken frustules parts [29]. Raw diatomite, as a carrier, often exhibits a disc-like shape, as evidenced by SEM images in the literature. The observable numerous pores of a regular diameter (in the 50–500 nm range) indicate high porosity of the material and its considerable size—the specific surface area, suitable for filling [30,49].

The SEM images presented in this paper (see Figure 4a,b; magnification 10  $\mu\text{m}$ ) show diatomaceous earth with an interesting cylindrical morphology. The cylinder-shaped elements (whole or broken) have regularly spaced holes, which makes them resemble a honeycomb. Identical observations were made by Slebi-Acevedo et al. (2021) [36] during their experiment. The highly porous structure of diatoms was also confirmed and described



in detail by Lutyński et al. (2019) [22]. Most of the frustule species were identified by the author as discoid frustules from the *Thalassiosiraceae* family and cylindric *Aulacoseira islandica*. The valve pore pattern is genome-encoded, as Tramontano et al. (2020) explain in their publication, species-specific, and forms an array called the areola, which propagates into the frustule depth and can be round, polygonal, or elongate [23].

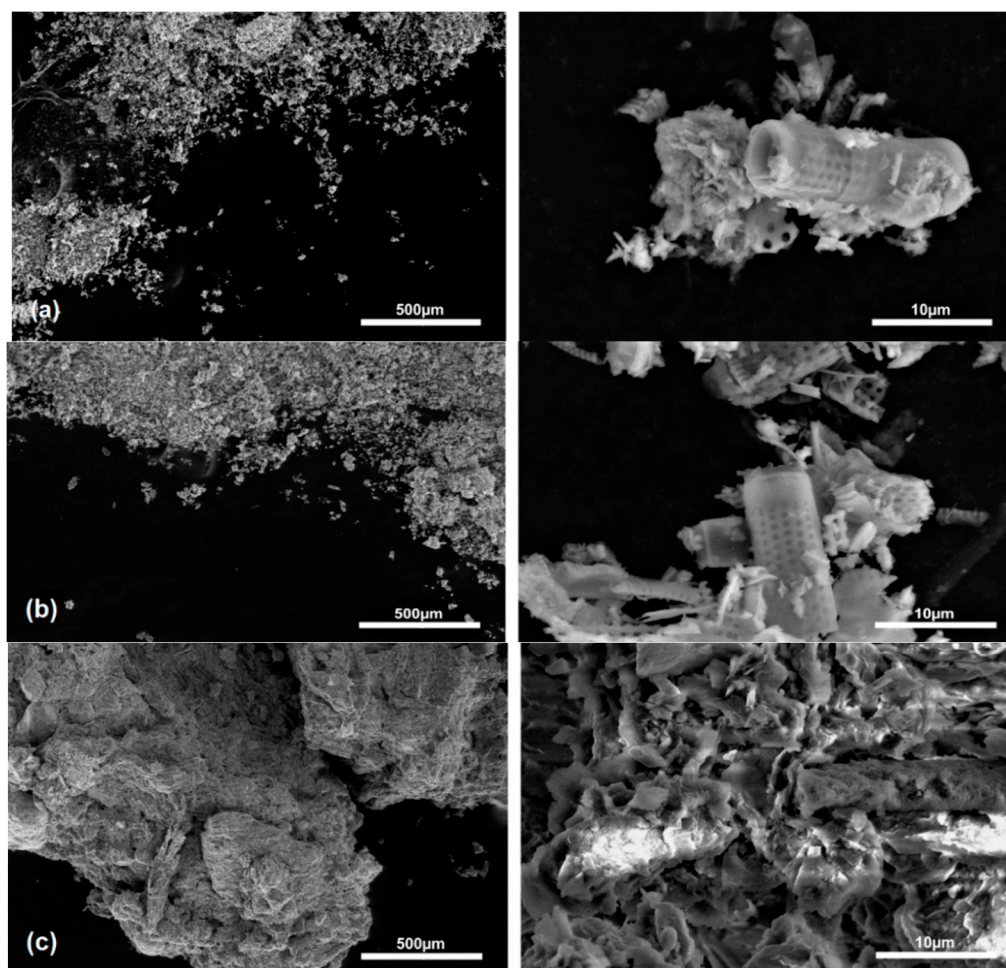


**Figure 4.** SEM images of (a) diatomaceous earth/peat carrier (DEP), (b) diatomaceous earth (DE), and (c) peat at different magnifications: 500 and 10 µm diameter particles.

The diatomite used in this study was 100% freshwater-derived commercial diatomaceous earth (amorphous silica), intended for consumption. Such powders are formed by calcination, conducted to separate water of crystallization and remove organic matter, followed by grinding and air classification [54,55]. It is worth mentioning the existence of a close relationship between the calcination temperature of porous materials and the physical and chemical properties that characterize them as well as, consequently, the type of their application [56].

In the SEM images presented in that study, the cylindrical forms of the diatomite have distinct pores (Figure 4b; magnification: 10 µm). The broken and crumbled parts were the result of grinding, which was one of the final stages of production. The SEM image of the diatomaceous earth/peat carrier system (Figure 4a; magnification: 10 µm) confirms the significance of peat in the carrier, which was partially distributed on DE, increasing the absorbency of the material for the cells and acting as a medium. According to data from the published literature, a sample of raw diatomite contains 90% of particles smaller than 33.5 µm [29]. Fu et al. (2015) [49] presented the particle size distribution of diatomaceous earth in his paper. According to the results of the analysis performed by Fu et al., the

particle size shows the trimodal distribution and the peak particle sizes are 0.58, 34.15, and 441.02  $\mu\text{m}$ . The diameter of 34.15  $\mu\text{m}$  corresponded to the base peak, which is consistent with the information reported by Janićijević et al. (2014) [29].

The second component of the carrier material used in this study was deacidified peat. Physicochemical analysis, including SEM analysis, was performed on material that was dried and crushed in a porcelain mortar to form a powder. The SEM image in Figure 4c (see Figure 4c; magnification 500 and 10  $\mu\text{m}$ ) shows an irregular and porous/rough microstructure. A similar peat morphology was presented by Paleckiene et al. (2021) [39]. This structure is more similar to a spongy fibrous structure (poorly decomposed peat) than to a fibrous specific structure (moderately decomposed peat). The spongy structure is formed by the undecomposed remains of peat-forming plants, which are easy to identify—these are moss peats [39].

Due to their fibrous structure, peats tend to vary in porosity (volume) depending on the moisture content. This phenomenon particularly intensifies during the winter period. The tendency of peat to expand is important for engineering reasons and it particularly applies to very cohesive soils containing a significant amount of clay particles. The high absorptiveness of peat with a fibrous spongy structure (Figure 4c; magnification 10  $\mu\text{m}$ ) is crucial for the protective function of peat, as a carrier, for soil bacteria [38]. Soil porosity, in turn, is widely recognized as the most important criterion for ensuring good soil aeration [57].

### 3.2.3. Adsorptive Properties

In order to determine the feasibility of using the diatomaceous earth/peat (3:1) system as a microbial carrier in the AD process, as well as to obtain information on the influence of both material components on the microstructural properties of the carrier, the porous structure properties of the individual materials were determined using the BET method (see Table 3).

**Table 3.** Porous structure properties of DEP carrier, diatomaceous earth, and peat.

Material	$A_{\text{BET}}$	$V_p$	$S_p$
	( $\text{m}^2 \text{g}^{-1}$ )	( $\text{cm}^3 \text{g}^{-1}$ )	(nm)
DEP carrier	36.01	0.081	11.55
diatomaceous earth (DE)	32.51	0.073	10.08
Peat (P)	1.20	0.004	18.83

DEP: diatomaceous earth/peat;  $A_{\text{BET}}$ : BET surface area;  $V_p$ : pore volume;  $S_p$ : pore size.

As indicated by the results of the analyses presented in Table 3, pure diatomite and the carrier material with peat addition are characterized by similar values of microstructure parameters:  $A_{\text{BET}}$  surface area development of 36.01 and 32.51  $\text{m}^2 \text{g}^{-1}$ , comparable pore volume of 0.811 and 0.732  $\text{cm}^3 \text{g}^{-1}$ , and average pore diameter of 11.55 and 10.08 nm for the DEP carrier and DE, respectively. It was also noted that despite its good sorption properties and significant average pore diameter (18.83 nm), the specific surface area of peat, as a natural sorbent, is small at 1.50  $\text{m}^2/\text{g}$ . The obtained values are consistent with the literature data [40]. Diatomite present in the DEP carrier sample in dominant amounts, similarly to peat, exhibits a nitrogen adsorption-desorption isotherm, i.e., type II isotherm with a H3-type hysteresis loop based on the recommendations of the International Union of Pure and Applied Chemistry, IUPAC (see Supplementary Materials, Figure S1a,b). Type II isotherms are obtained from non-porous or macroporous adsorbents [58,59].

The significant pore size of diatomite and peat, and the developed specific surface area of DE, as the main carrier component in the proposed material, enable the effective formation of durable biofilm layers [27]. The implementation of anaerobic digestion with DEP can therefore significantly increase the chances of survival and activity of bacterial cells, even under less stable process conditions.

### 3.2.4. Thermal Properties

Thermal analysis of diatomaceous earth, a soft rock consisting mainly of amorphous silica  $\text{SiO}_2$  and admixtures of crystalline silica, has been performed by many scientists before. The DTA-TG analysis (differential thermal analysis-thermogravimetry) conducted by Qian et al. (2015) and Fu et al. (2015) for diatomite also confirmed the excellent thermal stability of the material. The peaks in the TG curve, corresponding to temperature values of 76 and 170 °C described in the publications of those authors, were attributed to water loss probably from both diatomaceous silica and some clay impurities [30,49]. The recorded broad endothermic peak at 106 °C in the DTA curve was consistent with the TG findings and indicated the dehydration of the sample. Only at temperatures higher than 1000 °C, a phase transformation of diatomaceous silica from disordered opal-A structure to ordered  $\alpha$ -cristobalite can be expected [29]. In another study, Đặng et al. (2021) noted the bending points on TG curves, at around 433 °C for diatomite, and considered them most likely responsible for the dehydroxylation of silanol groups and evaporation of associated bounded water molecules [34].

Knowledge of the soil thermal properties is required when studying coupled heat and water transport across the vadose zone [60]. Thermal analysis of peat has already been performed by many other researchers and presented in several papers [61,62]. For peat, those studies are practically limited to the determination of mass loss due to dehydration and the processes of burning organic matter. The DTA curve shows the exothermic effect (related to heat release), with a maximum at temperatures above 450 °C. This effect is caused by the oxidation of the organic components of peat, dominant in its composition [61], and partly by the decomposition of the aromatic nucleus of humic acids [62]. The TG curve clearly shows that the highest mass loss in peat occurs in the temperature range of about 220–600 °C, and its final value stabilizes at about 84–87% mass loss.

The physical combination of two substances with high thermal stability creates a system with exactly those properties. Both the dominant DEP carrier component, i.e., diatomaceous earth and peat do not decompose in the temperature range of mesophilic or thermophilic methane fermentation and can act as a cell carrier in this process.

### 3.2.5. Determining the Microbial Biomass

In the analysis of the measurement of cellular biomass, cultured using the tested DEP carrier, an autochthonous Gram-positive sporulating strain of *Bacillus amyloliquefaciens* was used (see Supplementary Materials, Figure S2a,b). These microorganisms are generally aerobic, partially anaerobic, and characterized by a high degree of physiological and metabolic diversity, determined by genetic diversity [63]; they can survive in environments with a wide range of temperatures, pH, and salinity. The high growth rate of *Bacillus amyloliquefaciens* and its efficient system of synthesis and secretion of extracellular proteins were important reasons for choosing this particular strain for the test [64,65]. According to the literature, inoculation with *Bacillus cereus* of tea leaves biochar as a carrier improves soil fertility and crop yield. Such treatment did, in fact, enhance the proteobacteria (11%), firmicutes (46%), actinobacteria (20%), and cyanobacteria (33%) community as compared to peat alone [66].

The dominant component of the DEP carrier (3:1), diatomite, as one of the bioactive mesoporous silica materials (MSNs), has recently been undergoing advanced clinical trials testing its possible application in regenerative medicine. Diatomaceous earth attracts attention due to its adhesion, the ability to proliferate and differentiate bacterial cells, its characteristic surface, and highly porous 3D nanostructure, providing an alternative to the development of low-cost and innovative scaffolds. In her previous work, Pilarska et al., 2021, also highlighted the importance of the effect of pure silica on the methanogenic activity in the AD process, e.g., in sewage sludge [9].

The second component of the carrier under study, peat, as previously mentioned, is the base of many microbial inoculants used in agriculture [38]. As a material for carrying microorganisms, it has a number of properties ideal for this function, and at the same

time it increases cell proliferation and chances of survival of the microorganisms thanks to its bacterial protection properties. This fact was confirmed in studies involving peat as a carrier for legume bacteria (*Rhizobium leguminosarum* bv. *trifolii*) [67].

The bacterial cell biomass determined in this experiment in the culture grown with the use of diatomaceous earth/peat carrier (3:1) was  $9.35 \pm 0.03$  g/100 mL and it is a value slightly lower than the yield of the culture grown using the silica/ lignin system (4:1), presented in an earlier study [9]. Given the considerable cost of producing silica and lignin, choosing diatomite in combination with peat as a cell carrier for anaerobic biodegradation seems more reasonable.

### 3.3. Process Stability and Efficiency

The use of organic substrates of varying chemical compositions, including waste, on the one hand offers a wide potential for process implementation, but on the other it has its limitations related to the need for continuous monitoring of the AD process. Monitoring the physicochemical parameters of anaerobic degradation allows control and steering of the process itself. During the decomposition of biomass of varying chemical compositions, volatile fatty acids (VFA) may be rapidly released in the first stage of the process. This effect is often associated with high organic loading rates (OLR), occurring, for example, in the case of materials with a high carbohydrate and fat content, which contribute to a decrease in pH (acidification of the environment). The decrease in pH is preceded by an increase of SCFAs.

Volatile fatty acids/total alkalinity ratio is the most commonly used parameter for assessing process stability. Total alkalinity is a parameter showing the buffering capacity of the system. An increase in the VFA/TA ratio above 0.4 (indicating some destabilization of the decomposition) occurred only in the WF and WFC control samples. The addition of the DEP carrier was conducive to a stable process. The lowest VFA/TA ratio values were recorded for the WF + DEP sample. The optimum pH range for methanogen growth is 6.5–7.2 [48]. For the four fermented samples (see Figure 5), no drop in pH value below 6.5 was observed. On the other hand, an increase in pH up to a value of 7.7 was recorded, especially for samples containing cheese waste. The increase in pH, in the case of cheese waste and milk-filled wafers, may be the result of the breakdown of casein—a milk protein [3]. Increased alkalinity affects the  $\text{NH}_3$  and  $\text{NH}_4^+$  dissociation equilibrium.

Measurements of concentration of  $\text{N-NH}_4^+$  are important for the AD process implemented with the use of protein substrates and sewage sludge. The toxic effect of a compound depends, for most biological processes, on the amount, concentration, and form of the substance. In accordance with the critical values [48], the  $\text{N-NH}_4^+$  concentrations obtained for fermenting batches were maintained at acceptable levels, from  $151 \text{ mg L}^{-1}$ —for WF-control to  $1008 \text{ mg L}^{-1}$ —for WFC + DEP (see Supplementary Materials, Figure S3). The values of the released ammonium nitrogen were significantly higher for the systems with cheese waste.

The graphs labelled as Figure 6a,b show the cumulative volume of biogas and methane obtained for each sample, converted into VS (volatile solids)—Figure 6a and TS (total solids)—Figure 6b. The methane content of biogas ranged from 50.5% for WF-control to 51.9% for WFC + DEP. For the WF + DEP and WFC-control samples, the volume of methane was comparable and contributed 51.5 and 51.1%, respectively.

The volume of biogas, obtained from the WF-control sample, was  $705.16 \text{ m}^3 \text{ Mg}^{-1}$  VS in terms of volatile solids (VS) (see Figure 6a), while in terms of TS, contained in the waste wafers, it was lower, at  $510.61 \text{ m}^3 \text{ Mg}^{-1}$  TS. The chemical composition of confectionery waste has been previously described by Pilarska et al. (2018, 2019), who is one of the first researchers to address the fermentation of this type of waste [6,12]. As confirmed by the results of this author's research, the combination of waste wafers with dairy waste, including cheese waste, produces a synergistic effect in the form of increased enzyme activity and an increase in the number of cells responsible for the production of methane [6]. It seems that a slightly alkaline reaction facilitates decomposition of dairy materials, effectively buffers the



system, and is a source of good nutrient medium [3]. The aforementioned effect resulted, also in this study, in an increase of the methane production capacity from  $356.11 \text{ m}^3 \text{ Mg}^{-1}$  VS (WF) to  $413.91 \text{ m}^3 \text{ Mg}^{-1}$  VS (WFC).

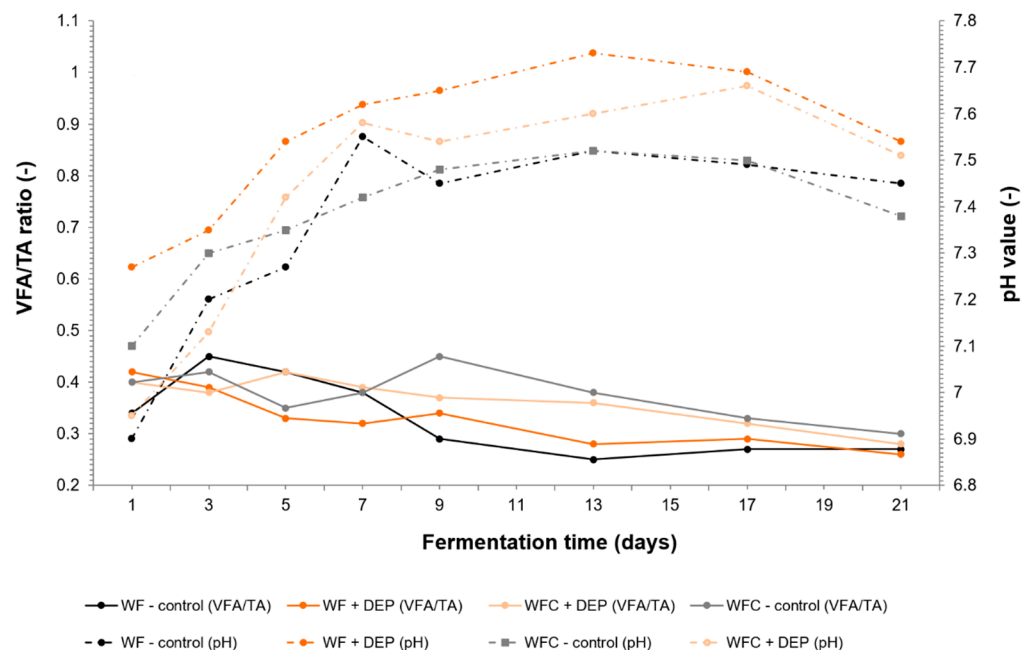


**Figure 5.** Variation in the pH and VFA/TA in the WF-control, WF + DEP, WFC-control, and WFC + DEP samples.

The addition of the DEP carrier system under study to the WF waste wafers increased the volume of the produced methane from  $356.11 \text{ m}^3 \text{ Mg}^{-1}$  VS to  $411.04 \text{ m}^3 \text{ Mg}^{-1}$  VS, while for the system with waste cheese, it was increased from  $413.46 \text{ m}^3 \text{ Mg}^{-1}$  VS to  $473.91 \text{ m}^3 \text{ Mg}^{-1}$  VS. This is a favorable result, comparable to/slightly higher than the Biochemical Methane Potential (BMP) of food wastes of a similar and different chemical composition to those tested [2,4,10,11]. The efficiency of biogas production from confectionery waste and cheese waste was verified in articles by Pilarska et al. (2018, 2019) [8,12].

Due to the functional properties of both substances: the microstructural properties of diatomite and the sorption properties of peat, the hybrid (3:1) proved to be an excellent cell carrier for anaerobic digestion. Potentially, strongly conductive diatomaceous earth can act as an electron transporter, contributing to the increase of electron transfer efficiency in methane production. Previous work has also demonstrated that silica adsorbs proteins (concept of differential protein adsorption) and that it also stimulates protein proliferation [68,69]. For diatomaceous earth/peat (3:1), the increase in biogas production capacity was about 13%, while the addition of silica/lignin (4:1) resulted in about an 18% increase in the volume of gas produced. However, given the cost of producing synthetic silica and lignin, either by synthesis or by recovery from waste materials, using a combination of relatively cheap diatomite and peat is a more economical and environmentally friendly solution. The results of enzyme activity, discussed in the next subsection, clearly indicate a positive effect of the applied carrier materials on the functioning of the microorganisms catalyzing biomass decomposition in the WF and WFC samples.



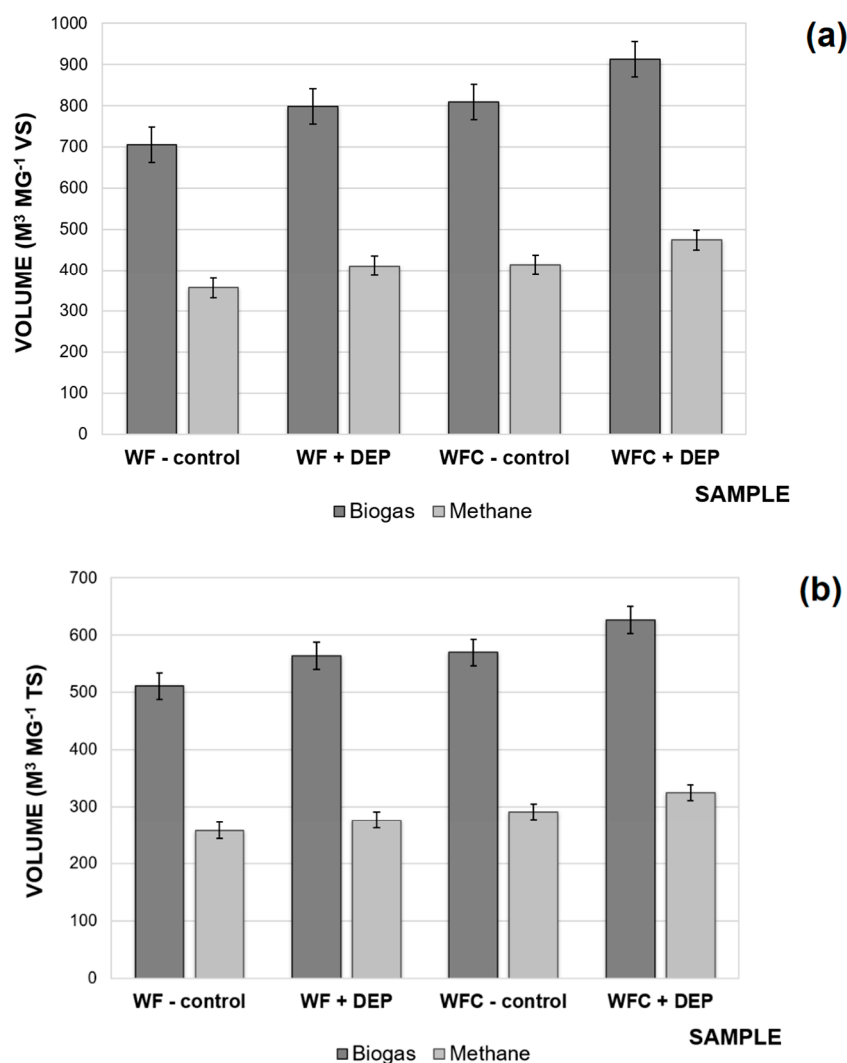


**Figure 6.** Biogas and methane efficiency from Mg of (a) volatile solids (VS) and (b) total solids (TS) obtained from WF-control, WF + DEP, WFC-control, and WFC + DEP samples.

### 3.4. Dehydrogenase Activity

Based on the performed statistical analysis, it was shown that the level of dehydrogenase activity in the fermentation samples of food waste varied significantly based on the date of sampling, as well as the type of experimental variant (see Figure 7). Wafer waste with added cheese (WFC-control sample) and with cheese and carrier (WFC + DEP sample) proved to be a good environment for the growth of an autochthonous microbiome, which translated into higher levels of dehydrogenases (DHA).

In their previous publications, Pilarska et al. (2020) and Pilarska et al. (2021) also reported a significant increase in DHA activity in fermented waste wafer/cheese mixtures following the addition of a silica/lignin carrier system [9,21]. According to Guergoletto et al. (2017), running fermentation processes with the use of carriers has actual technological and economic benefits [70]. Immobilization of microbial cells on carriers, according to Qiu et al. (2019), is conducive to increasing their density per unit volume of the fermenter, leading to better substrate utilization and thus higher process efficiency and productivity [71].

The present study showed that the addition of a diatomaceous earth/peat carrier system contributed to a statistically significant increase in dehydrogenase activity, both in wafer waste fermented with cheese and without it. According to Lutyński et al. (2019) [22] and Benkacem et al. (2016) [27], diatomite is mainly composed of silica-containing phases (quartz, opal) and clay minerals (illite and kaolinite), which, according to the aforemen-

tioned authors, explains its high sorption capacity, cation exchange capacity, and adsorption properties, e.g., in relation to microorganisms. Furthermore, dehydrogenases are intracellular enzymes, produced mainly by living microorganisms, which show optimum activity in neutral or slightly alkaline environments [72]. This was also the reaction that accompanied the decomposition process conducted in the present study (see Figure 5). Similar observations were made by Pilarska et al. (2021), who pointed to a positive effect of the pH value of fermented food waste on DHA activity. However, the authors obtained a higher level of activity of the tested enzymes after using the silica/lignin carrier, compared to when using the DEP carrier, which also translated into a slightly higher biogas/methane production efficiency [73].

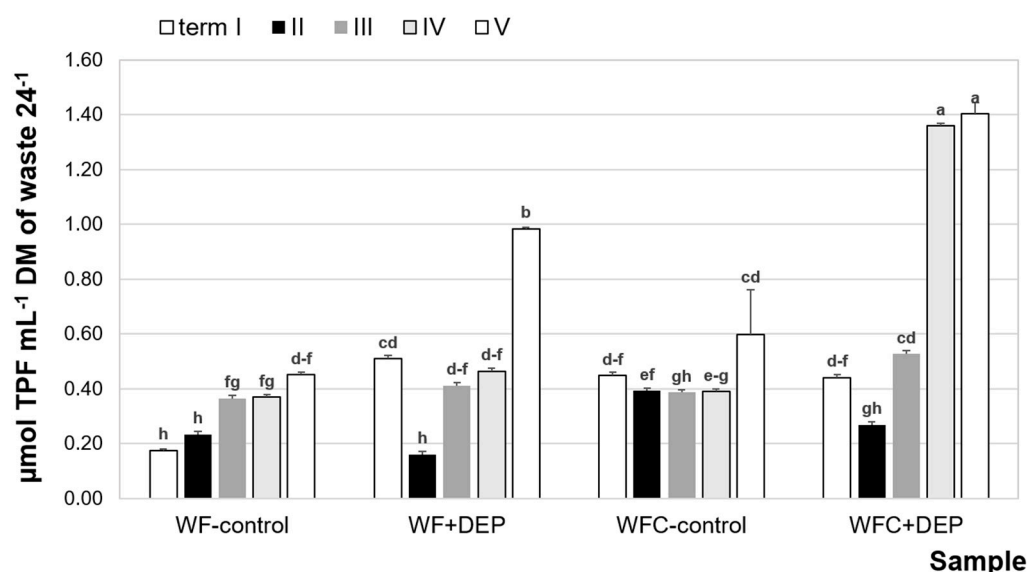


**Figure 7.** Dehydrogenase activity changes in the digested material. Explanation: the same letter indicates a lack of significant differences ( $p < 0.05$ ).

Many researchers have previously confirmed in their studies that the pH of fermented waste is one of the main parameters determining the activity of methane microorganisms [23,34,74]. The optimum pH value for their growth and development is between 6.6 and 7.6. Below pH 6.2, the growth and activity of microorganisms is inhibited by undissociated fatty acids that are thought to freely permeate the cellular membrane of microorganisms. After permeating the membrane, the fatty acids internally dissociate, thus lowering the cytoplasmic pH and affecting bacterial metabolism.

Principal component analysis (PCA) confirmed a significant effect of pH value on both DHA activity and the amount of biogas produced (Figure 8). The strongest positive correlations between pH value and biogas emissions were recorded for the variants with the addition of cheese:

1. Biogas emission (WFC-control) =  $818.95 \text{ pH}^2 - 5459.1$ ,  $R^2 = 0.53$
2. Biogas emission (WFC + DEP) =  $595.59 \text{ pH}^2 - 3830.2$ ,  $R^2 = 0.79$

Analyzing the results presented in Figure 7, the highest dehydrogenase activity was observed in most experimental variants (except WF-control) in the fifth term of analysis, while the lowest level of DHA was observed in the second term. The decrease in the activity of the analyzed enzymes in the second term of analyses could be due to the presence of inhibitors appearing during the decomposition of fermented raw materials, in this case, for example, ammonium ions released from samples containing cheese waste. In the second term, the lowest increase in  $\text{NH}_4^+$  content was shown in the WF-control variant (Figure S3 Supplementary Materials), which translated into stimulation of the activity of the enzymes tested in the present facility (Figure 7). In general, the process was stable, as confirmed

by the changes in the value of the VFA/TA ratio parameter, which is important for the monitoring of the AD process.

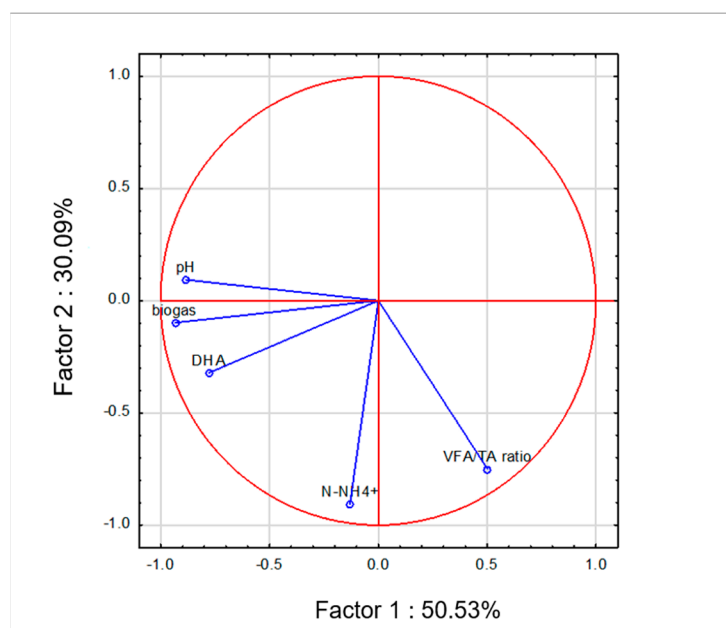


**Figure 8.** Distribution of bacteria activity and chemical parameters in two PCA axes. Legend: DHA—dehydrogenase activity, VFA/TA ratio—volatile fatty acids-to-total alkalinity ratio, N-NH<sub>4</sub><sup>+</sup>—ammonium nitrate.

#### 4. Conclusions

The microbial carrier, diatomaceous earth/peat, as proven by the results of the performed experiments, is characterized by high porosity due to the presence of both components, as well as a highly developed specific surface area due to the significant proportion of diatomite. The proposed carrier, as a material of natural origin, is environmentally friendly, biocompatible, and cheap. The dominant component of the DEP carrier (3:1), diatomite, as a bioactive mesoporous silica material, as well as porous peat, increase cell proliferation.

Based on the studies, the addition of the diatomaceous earth/peat system contributed to an increase in the activity of dehydrogenases, both in the case of waste wafers fermented without the addition of cheese (WF + DEP) and with cheese (WFC + DEP). This effect translates into biogas/methane yield from those samples—an increase in the volume of produced biogas was recorded for samples fermented with DEP carrier: for WF + DEP by 13.18% to a cumulative methane yield of 411.04 m<sup>3</sup> Mg<sup>−1</sup> VS, while for WFC + DEP by 12.85% to 473.91 m<sup>3</sup> Mg<sup>−1</sup> VS. The monitoring of the process stability control parameters did not show any significant signals of destabilization of the AD process for any of the samples.

The positive effect of the diatomaceous earth/peat carrier, as a new microbial additive for anaerobic digestion, was confirmed by the increased biomass conversion, the diatomaceous earth/peat carrier was confirmed by the increased biomass conversion rate, the reduction of the retention time, and the improved efficiency of the process, which allows for considering the application of DEP as an effective and economical technology, dedicated to the AD of organic substrates. In the second part of the study, interesting results will be presented on quantitative and qualitative changes in genetic diversity of bacterial communities in anaerobic bioreactors as a result of the application of a diatomaceous earth/peat cell carrier.

**Supplementary Materials:** The following supporting information can be downloaded at: <https://www.mdpi.com/article/10.3390/en15093442/s1>, Figure S1: (a) N<sub>2</sub> adsorption/desorption isotherms and (b) pore size distribution of the diatomaceous earth (DE) and peat; Figure S2: (a) A *Bacillus*

*amyloliquefaciens* culture with the diatomaceous earth/peat system, (b) SEM image of cell *B. amyloliquefaciens* colonisation; Figure S3: Changes in the  $\text{N-NH}_4^+$  during the anaerobic digestion of the WF-control, WF+DEP, WFC-control and WFC+DEP samples; Table S1: Elemental content of diatomaceous earth (DE) and peat (P).

**Author Contributions:** Conceptualization, A.A.P.; Methodology, A.A.P., A.W.-M. and M.A.; Software, K.P., M.A. and M.Z.; Validation, D.C.-S., M.A., M.Z. and A.N.; Formal analysis, A.A.P., D.C.-S. and M.Z.; Investigation, A.A.P., A.W.-M., K.P. and M.A.; Resources, A.A.P., A.W.-M. and A.N.; Data curation, A.A.P., D.C.-S. and A.W.-M.; Writing—original draft preparation, A.A.P.; Writing—review and editing, A.A.P. and A.W.-M.; Visualization, A.A.P., A.W.-M., K.P. and M.Z.; Supervision, D.C.-S. and A.N.; Project administration, A.A.P. and D.C.-S.; Funding acquisition, A.A.P. All authors have read and agreed to the published version of the manuscript.

**Funding:** This research was funded by the National Science Centre, Poland (grant no. DEC-2019/03/ST8/01867).

**Institutional Review Board Statement:** Not applicable.

**Informed Consent Statement:** Not applicable.

**Conflicts of Interest:** The authors declare no conflict of interest.

## References

1. Kuo, J.; Dow, J. Biogas production from anaerobic digestion of food waste and relevant air quality implications. *J. Air Waste Manag. Assoc.* **2017**, *67*, 1000–1011. [\[CrossRef\]](#) [\[PubMed\]](#)
2. Xu, F.; Li, Y.; Ge, X.; Yang, L.; Li, Y. Anaerobic digestion of food waste—Challenges and opportunities. *Bioresour. Technol.* **2018**, *247*, 1047–1058. [\[CrossRef\]](#) [\[PubMed\]](#)
3. Pilarska, A.A.; Pilarski, K.; Witaszek, K.; Waliszewska, H.; Zborowska, M.; Waliszewska, B.; Kolasiński, M.; Szwarc-Rzepka, K. Treatment of dairy waste by anaerobic digestion with sewage sludge. *Ecol. Chem. Eng. S* **2016**, *23*, 99–115. [\[CrossRef\]](#)
4. Pilarska, A.A.; Pilarski, K.; Ryniecki, A.; Tomaszuk, K.; Dach, J.; Wolna-Maruwka, A. Utilization of vegetable dumplings waste from industrial production by anaerobic digestion. *Int. Agrophys.* **2017**, *31*, 93–102. [\[CrossRef\]](#)
5. Mehariya, S.; Patel, A.K.; Obulisamy, P.K.; Punniyakotti, E.; Jonathan, W.C.; Wong, J.W.C. Co-digestion of food waste and sewage sludge for methane production: Current status and perspective. *Bioresour. Technol.* **2018**, *265*, 519–531. [\[CrossRef\]](#) [\[PubMed\]](#)
6. Pilarska, A.A. Anaerobic co-digestion of waste wafers from the confectionery production with sewage sludge. *Pol. J. Environ. Stud.* **2018**, *27*, 237–245. [\[CrossRef\]](#)
7. Xie, S.; Wickham, R.; Nghiem, L.D. Synergistic effect from anaerobic co-digestion of sewage sludge and organic wastes. *Int. Biodeter. Biodegrad.* **2017**, *116*, 191–197. [\[CrossRef\]](#)
8. Pilarska, A.A.; Wolna-Maruwka, A.; Pilarski, K.; Janczak, D.; Przybył, K.; Gawrysiak-Witulska, M. The use of lignin as a microbial carrier in the co-digestion of cheese and wafer waste. *Polymers* **2019**, *11*, 2073. [\[CrossRef\]](#)
9. Pilarska, A.A.; Wolna-Maruwka, A.; Niewiadomska, K.; Pilarski, K.; Adamski, M.; Grzyb, A.; Grządziel, J.; Gałazka, A. Silica/lignin carrier as a factor increasing the process performance and genetic diversity of microbial communities in laboratory-scale anaerobic digesters. *Energies* **2021**, *14*, 4429. [\[CrossRef\]](#)
10. Lafitte-Trouqué, S.; Forster, C.F. Dual anaerobic co-digestion of sewage sludge and confectionery waste. *Bioresour. Technol.* **2000**, *71*, 77–82. [\[CrossRef\]](#)
11. Rusín, J.; Kašáková, K.; Chamrádová, K. Anaerobic digestion of waste wafer material from the confectionery production. *Energy* **2015**, *85*, 194–199. [\[CrossRef\]](#)
12. Pilarska, A.A.; Pilarski, K.; Wolna-Maruwka, A.; Boniecki, P.; Zaborowicz, M. Use of confectionery waste in biogas production by the anaerobic digestion process. *Molecules* **2019**, *24*, 37. [\[CrossRef\]](#) [\[PubMed\]](#)
13. Guisan, J.M. *Methods in Biotechnology: Immobilization of Enzymes and Cells*; Humana Press: Totowa, NJ, USA, 2006.
14. Lalov, I.G.; Krysteva, M.A.; Phelouzat, J.L. Improvement of biogas production from vinasse via covalently immobilized methanogens. *Bioresour. Technol.* **2001**, *79*, 83–85. [\[CrossRef\]](#)
15. Pilarska, A.A.; Wolna-Maruwka, A.; Pilarski, K. Kraft lignin grafted with polyvinylpyrrolidone as a novel microbial carrier in biogas production. *Energies* **2018**, *11*, 3246. [\[CrossRef\]](#)
16. Pilarska, A.A.; Pilarski, K.; Wolna-Maruwka, A. Cell immobilization on lignin–polyvinylpyrrolidone material used for anaerobic digestion of waste wafers and sewage sludge. *Environ. Eng. Sci.* **2019**, *36*, 478–490. [\[CrossRef\]](#)
17. Dzionek, A.; Wojcieszynska, D.; Guzik, U. Natural carriers in bioremediation: A review. *Electron. J. Biotechnol.* **2016**, *23*, 28–36. [\[CrossRef\]](#)
18. Weiß, S.; Zankel, A.; Lebuhn, M.; Petrak, S.; Somitsch, W.; Guebitz, G.M. Investigation of microorganisms colonising activated zeolites during anaerobic biogas production from grass silage. *Bioresour. Technol.* **2011**, *102*, 4353–4359. [\[CrossRef\]](#)
19. Chauhan, A.; Ogram, A. Evaluation of support matrices for immobilization of anaerobic consortia for efficient carbon cycling in waste regeneration. *Biochem. Biophys. Res. Commun.* **2005**, *327*, 884–893. [\[CrossRef\]](#)

20. Seelert, T.; Ghosh, D.; Yargeau, V. Improving biohydrogen production using *Clostridium beijerinckii* immobilized with magnetite nanoparticles. *Appl. Microbiol. Biotechnol.* **2015**, *99*, 4107. [\[CrossRef\]](#)
21. Pilarska, A.A.; Wolna-Maruwka, A.; Niewiadomska, A.; Pilarski, K.; Olesienkiewicz, A. A Comparison of the influence of kraft lignin and the kraft lignin/silica system as cell carriers on the stability and efficiency of the anaerobic digestion proces. *Energies* **2020**, *13*, 5803. [\[CrossRef\]](#)
22. Lutyński, M.; Sakiewicz, P.; Lutyńska, S. Characterization of diatomaceous earth and halloysite resources of Poland. *Minerals* **2019**, *9*, 670. [\[CrossRef\]](#)
23. Tramontano, C.; Chianese, G.; Terracciano, M.; de Stefano, L.; Rea, I. Nanostructured biosilica of diatoms: From water world to biomedical applications. *Appl. Sci.* **2020**, *10*, 6811. [\[CrossRef\]](#)
24. Sardo, A.; Orefice, I.; Balzano, S.; Barra, S.; Romano, G. Mini-review: Potential of diatom-derived silica for biomedical applications. *Appl. Sci.* **2021**, *11*, 4533. [\[CrossRef\]](#)
25. Thangaraj, S.; Sun, J. The biotechnological potential of the marine diatom *Skeletonema dohrnii* to the elevated temperature and pCO<sub>2</sub>. *Mar. Drugs* **2020**, *18*, 259. [\[CrossRef\]](#) [\[PubMed\]](#)
26. Delasoie, J.; Zobi, F. Natural diatom biosilica as microshuttles in drug delivery systems. *Pharmaceutics* **2019**, *11*, 537. [\[CrossRef\]](#)
27. Benkacem, T.; Hamdi, B.; Chamayou, A.; Balard, H.; Calvet, R. Physicochemical characterization of a diatomaceous upon an acid treatment: A focus on surface properties by inverse gas chromatography. *Powder Technol.* **2016**, *294*, 498–507. [\[CrossRef\]](#)
28. Hussein, H.A.; Abdullah, M.A. Anticancer compounds derived from marine diatoms. *Mar. Drugs* **2020**, *18*, 356. [\[CrossRef\]](#)
29. Janičević, J.; Krajišnik, D.; Čalić, B.; Vasiljević, B.N.; Dobričić, V.; Daković, A.; Antonijević, M.D.; Milić, J. Modified local diatomite as potential functional drug carrier—A model study for diclofenac sodium. *Int. J. Pharm.* **2015**, *496*, 466–474. [\[CrossRef\]](#)
30. Qian, T.; Li, J.; Min, X.; Deng, Y.; Guan, W.; Ning, L. Diatomite: A promising natural candidate as carrier material for low, middle and high temperature phase change material. *Energy Convers. Manag.* **2015**, *98*, 34–45. [\[CrossRef\]](#)
31. Zhang, Y.; Yu, Z.; Hu, Y.; Song, C.; Li, F.; He, W.; Wang, X.; Li, Z.; Lin, H. Immobilization of nitrifying bacteria in magnetic PVA-SA-diatomite carrier for efficient removal of NH-N from effluents. *Environ. Technol. Innov.* **2021**, *22*, 101407. [\[CrossRef\]](#)
32. Saidi, T.; Hasan, M. The effect of partial replacement of cement with diatomaceous earth (DE) on the compressive strength and absorption of mortar. *J. King Saud Univ. Eng. Sci.* **2020**, in press. [\[CrossRef\]](#)
33. Korunić, Z. Diatomaceous Earths—Natural Insecticides. *Pestic. Phytomed.* **2013**, *28*, 77–95. [\[CrossRef\]](#)
34. Đặng, T.H.; Nguyễn, X.H.; Chou, C.L.; Chen, B.H. Preparation of cancrinite-type zeolite from diatomaceous earth as transesterification catalysts for biodiesel production. *Renew. Energy* **2021**, *174*, 347–358.
35. Basri, H.F.; Anuar, A.N.; Yuzir, A.; Ab Halim, M.H. Diatomite carrier for rapid formation of aerobic granular sludge. *IOP Conf. Ser. Earth Environ. Sci.* **2020**, *479*, 012028. [\[CrossRef\]](#)
36. Slebi-Acevedo, C.J.; Zuluaga-Astudillo, D.A.; Ruge, J.C.; Castro-Fresno, D. Influence of the diatomite specie on the peak and residual shear strength of the fine-grained soil. *Appl. Sci.* **2021**, *11*, 1352. [\[CrossRef\]](#)
37. Zhang, Y.T.; Wei, W.; Wang, Y.; Ni, B.J. Enhancing methane production from algae anaerobic digestion using diatomite. *J. Clean. Prod.* **2021**, *315*, 128138. [\[CrossRef\]](#)
38. Albareda, M.; Rodríguez-Navarro, D.N.; Camacho, M.; Temprano, F.J. Alternatives to peat as a carrier for rhizobia inoculants: Solid and liquid formulations. *Soil Biol. Biochem.* **2008**, *40*, 2771–2779. [\[CrossRef\]](#)
39. Paleckiene, R.; Navikaite, R.; Slinksiene, R. Peat as a raw material for plant nutrients and humic substances. *Sustainability* **2021**, *13*, 6354. [\[CrossRef\]](#)
40. Bartczak, B.; Norman, M.; Klapiszewski, Ł.; Karwańska, N.; Kawalec, M.; Baczyńska, M.; Wysokowski, M.; Zdarta, J.; Ciesielczyk, F.; Jesionowski, T. Removal of nickel(II) and lead(II) ions from aqueous solution using peat as a low-cost adsorbent: A kinetic and equilibrium study. *Arab. J. Chem.* **2018**, *11*, 1209–1222. [\[CrossRef\]](#)
41. Michel, J.C. The physical properties of peat: A key factor for modern growing media. *Mires Peat* **2010**, *6*, 1–6.
42. Lee, S.Y.; Kim, E.G.; Park, J.R.; Ryu, Y.H.; Moon, W.; Park, G.H.; Ubaidillah, M.; Ryu, N.S.; Kim, K.M. Effect on chemical and physical properties of soil each peat moss, elemental sulfur, and sulfur-oxidizing bacteria. *Plants* **2021**, *10*, 1901. [\[CrossRef\]](#) [\[PubMed\]](#)
43. Norm VDI 4630; Fermentation of Organic Materials Characterization of the Substrate, Sampling, Collection of Material Data, Fermentation Tests. German Engineers Club: Düsseldorf, Germany, 2006.
44. DIN Guideline 38 414-S8; Characterisation of the Substrate, Sampling, Collection of Material Data, Fermentation Tests. German Institute for Standardization: Berlin, Germany, 1985.
45. Pilarska, A.A.; Pilarski, K.; Waliszewska, B.; Zborowska, M.; Witaszek, K.; Waliszewska, H.; Kolasiński, M.; Szwarc-Rzepka, K. Evaluation of bio-methane yields for high-energy organic waste and sewage sludge: A pilot-scale study for a wastewater treatment plant. *Environ. Eng. Manag. J.* **2019**, *18*, 2019–2030. [\[CrossRef\]](#)
46. Camiña, F.; Trasar-Cepeda, C.; Gil-Sotres, F.; Leirós, C. Measurement of dehydrogenase activity in acid soils rich in organic matter. *Soil Biol. Biochem.* **1998**, *30*, 1005–1011. [\[CrossRef\]](#)
47. Szaja, A.; Montusiewicz, A. Enhancing the co-digestion efficiency of sewage sludge and cheese whey using brewery spent grain as an additional substrate. *Bioresour. Technol.* **2019**, *291*, 121863. [\[CrossRef\]](#)
48. Chen, J.L.; Ortiz, R.; Steele, T.W.J.; Stuckey, D.C. Toxicants inhibiting anaerobic digestion: A review. *Biotechnol. Adv.* **2014**, *32*, 1523–1534. [\[CrossRef\]](#)



49. Fu, X.; Liu, Z.; Xi, Y.; Wang, J.; Lei, J. Preparation and properties of lauric acid/diatomite composites as novel form-stable phase change materials for thermal energy storage. *Energy Build.* **2015**, *104*, 244–249. [\[CrossRef\]](#)
50. Xu, B.; Li, Z. Paraffin/diatomite composite phase change material incorporated cement-based composite for thermal energy storage. *Appl. Energy* **2013**, *105*, 229–237. [\[CrossRef\]](#)
51. Gulturk, E.; Guden, M. Thermal and acid treatment of diatom frustules. *J. Achiev. Mater. Manuf. Eng.* **2011**, *46*, 196–203.
52. Cannavo, P.; Hafidhi, H.; Michel, J.C. Impact of root growth on the physical properties of peat substrate under a constant water regimen. *Hort. Sci.* **2011**, *46*, 1394–1399. [\[CrossRef\]](#)
53. Cortizas, A.M.; López-Merino, L.; Silva-Sánchez, N.; Sjöström, J.K.; Kylander, M.E. Investigating the mineral composition of peat by combining FTIR-ATR and multivariate analysis. *Minerals* **2021**, *11*, 1084. [\[CrossRef\]](#)
54. Pilarska, A.; Linda, I.; Wysokowski, M.; Pauksza, D.; Jesionowski, T. Synthesis of  $Mg(OH)_2$  from a magnesium salt and  $NH_4OH$  with direct functionalisation with poly(ethylene glycols). *Physicochem. Probl. Miner. Process.* **2012**, *48*, 631–643.
55. Pilarska, A.; Nowacka, M.; Pilarski, K.; Pauksza, D.; Klapiszewski, Ł.; Jesionowski, T. Preparation and characterisation of unmodified and modified with poly(ethylene glycol) magnesium hydroxide. *Physicochem. Probl. Miner. Process.* **2013**, *49*, 701–712.
56. Pilarska, A.; Markiewicz, E.; Ciesielczyk, F.; Jesionowski, T. The influence of spray drying on dispersive the and physicochemical properties of magnesium oxide. *Drying Technol.* **2011**, *29*, 1210–1218. [\[CrossRef\]](#)
57. Cannavo, P.; Michel, J.C. Peat particle size effects on spatial root distribution, and changes on hydraulic and aeration properties. *Sci. Hortic.* **2013**, *151*, 11–21. [\[CrossRef\]](#)
58. Rouquerol, F.; Rouquerol, J.; Sing, K. *Adsorption by Powders and Porous Solids*, 2nd ed.; Academic Press: London, UK, 1999.
59. Tsai, W.T.; Hsien, K.J.; Lai, C.W. Chemical activation of spent diatomaceous earth by alkaline etching in the preparation of mesoporous adsorbents. *Ind. Eng. Chem. Res.* **2004**, *43*, 7513–7520. [\[CrossRef\]](#)
60. Zhao, Y.; Si, B. Thermal properties of sandy and peat soils under unfrozen and frozen conditions. *Soil Tillage Res.* **2019**, *189*, 64–72. [\[CrossRef\]](#)
61. Grabowska-Olszewska, B. *Methods of Testing Cohesive Soils*; Geological Publishing: Warsaw, Poland, 1990.
62. Schnitzer, M.; Khan, S.U. *Soli Organic Matter*; Elsevier Scientific Publishing Company: Amsterdam, The Netherlands, 1978.
63. Bhatt, B.; Prajapati, V.; Patel, K.; Trivedi, U. Kitchen waste for economical amylase production using *Bacillus amyloliquefaciens* KCP2. *Biocatal. Agric. Biotechnol.* **2020**, *26*, 101654. [\[CrossRef\]](#)
64. Karunakaran, G.; Suriyaprabha, R.; Manivasakan, P.; Yuvakkumar, R.; Rajendran, V.; Prabhu, P.; Kannan, N. Effect of nanosilica and silicon sources on plant growth promoting rhizobacteria, soil nutrients and maize seed germination. *IET Nanobiotechnol.* **2013**, *7*, 70–77. [\[CrossRef\]](#)
65. Deb, P.; Talukdar, S.A.; Mohsina, K.; Sarker, P.K.; Sayem, S.M.A. Production and partial characterization of extracellular amylase enzyme from *Bacillus amyloliquefaciens* P-001. *SpringerPlus* **2013**, *2*, 154. [\[CrossRef\]](#)
66. Azeem, M.; Ul Hassan, T.; Tahir, M.I.; Ali, A.; Jeyasundar, P.G.S.A.; Hussain, Q.; Bashir, S.; Mehmood, S.; Zhang, Z. Tea leaves biochar as a carrier of *Bacillus cereus* improves the soil function and crop productivity. *Appl. Soil Ecol.* **2021**, *157*, 103732. [\[CrossRef\]](#)
67. Rachwał, K.; Boguszevska, A.; Kopcińska, J.; Karaś, M.; Tchórzewski, M.; Janczarek, M. The regulatory protein *rosR* affects *Rhizobium leguminosarum* bv. *trifolii* protein profiles, cell surface properties, and symbiosis with clover. *Front. Microbiol.* **2016**, *23*, 1302. [\[CrossRef\]](#) [\[PubMed\]](#)
68. Saikia, J.; Yazdimamaghani, M.; Moghaddam, S.P.H.; Ghandehari, H. Differential protein adsorption and cellular uptake of silica nanoparticles based on size and porosity. *ACS Appl. Mater. Interfaces* **2016**, *8*, 34820–34832. [\[CrossRef\]](#) [\[PubMed\]](#)
69. Gondim, D.R.; Cecilia, J.A.; Rodrigues, T.N.B.; Vilarrasa-García, E.; Rodríguez-Castellón, E.; Azevedo, D.C.S.; Silva, I.J., Jr. Protein Adsorption onto Modified Porous Silica by Single and Binary Human Serum Protein Solutions. *Int. J. Mol. Sci.* **2021**, *22*, 9164. [\[CrossRef\]](#) [\[PubMed\]](#)
70. Guergoletto, K.B.; Busanello, M.; Garcia, S. Influence of carrier agents on the survival of *Lactobacillus reuteri* LR92 and the physicochemical properties of fermented juçara pulp produced by spray drying. *LWT* **2017**, *80*, 321–327. [\[CrossRef\]](#)
71. Qiu, L.; Deng, Y.F.; Wang, F.; Davaritouchaee, M.; Yao, Y.Q. A review on biochar-mediated anaerobic digestion with enhanced methane recovery. *Renew. Sust. Energy Rev.* **2019**, *115*, 109373. [\[CrossRef\]](#)
72. Sánchez, J.B.; Alonso, J.Q.; Oviedo, M.C. Use of microbial activity parameters for determination of a biosolid stability index. *Bioresour. Technol.* **2006**, *97*, 562–568. [\[CrossRef\]](#)
73. Poirier, S.; Chapleur, O. Influence of support media supplementation to reduce the inhibition of anaerobic digestion by phenol and ammonia: Effect on degradation performances and microbial dynamics. *Data Br.* **2018**, *19*, 1733–1754. [\[CrossRef\]](#)
74. Kotarska, K.; Dziemianowicz, W.; Świerczyńska, A. The effect of detoxification of lignocellulosic biomass for enhanced methane production. *Energies* **2021**, *14*, 5650. [\[CrossRef\]](#)